

A potential vorticity perspective on the motion of a mid-latitude winter storm

G. Rivière,¹ P. Arbogast,¹ G. Lapeyre,² and K. Maynard¹

Received 24 May 2012; revised 1 June 2012; accepted 6 June 2012; published 30 June 2012.

[1] The motion of mid-latitude surface cyclones relative to the jet streams is of particular interest because of the commonly observed strong and rapid deepening they undergo when they cross the upper-level jet axis. The purpose of the present study is to validate a recent theory that may explain this motion which is a generalization of the so-called beta drift in the mid-latitude baroclinic context. According to this theory, the key parameter controlling the movement of a surface cyclone across the mean tropospheric jet is the vertically averaged potential vorticity (PV) gradient associated with the jet. To test this theoretical result, numerical sensitivity experiments are performed using the Météo-France global operational forecast model ARPEGE-IFS for the particular case of the storm Xynthia (26–28 February 2010). The control forecast, starting from the operational analysis almost 2 days before the storm hit France, represents the trajectory of the storm quite well, together with the deepening during the crossing of the upper-level jet axis. A PV-inversion tool is used to modify the vertically averaged PV gradient of the initial state. As expected from the theory, when the PV gradient is intensified, there is a quicker displacement of the surface cyclone toward the jet axis and the jet-crossing phase occurs earlier than in the control forecast. The opposite occurs for a reduced PV gradient. The interpretation is that an enhanced PV gradient reinforces the dipolar PV anomaly located at upper levels which, in turn, advects the surface cyclone faster towards the jet axis. **Citation:** Rivière, G., P. Arbogast, G. Lapeyre, and K. Maynard (2012), A potential vorticity perspective on the motion of a mid-latitude winter storm, *Geophys. Res. Lett.*, *39*, L12808, doi:10.1029/2012GL052440.

1. Introduction

[2] It is well-known that storm tracks as defined by 2–6 day band-pass filtered geopotential height mainly lie on the poleward side of the jet streams [Blackmon *et al.*, 1984; Wallace *et al.*, 1988] and that cyclone tracks are rapidly deflected poleward on the downstream side of the oceanic basins [Hoskins and Hodges, 2002]. Furthermore, many intense Atlantic cyclones cross the upper-level jet from its warm- to its cold-air side, where they deepen rapidly, creating damaging wind storms farther downstream in Europe [Rivière and Joly, 2006; Pinto *et al.*, 2009].

[3] The poleward deflection relative to the mean flow of mid-latitude cyclones has not yet been explained to our knowledge. However, Gilet *et al.* [2009] have recently proposed a potential mechanism consisting of a generalization of the so-called beta drift in a mid-latitude baroclinic context. This nonlinear phenomenon was first introduced by Rossby [1948] and Adem [1956] in a barotropic context to better understand the motion of atmospheric vortices in the tropics and mid-latitudes. Since then, it has been extensively studied to analyze the displacement of tropical cyclones [Holland, 1983; Wang *et al.*, 1997] and oceanic vortices [McWilliams and Flierl, 1979; Carton, 2001] but, curiously, not at all that of extratropical cyclones. The beta drift can be easily understood by considering the time evolution of an initially symmetric vortex on a β -plane (i.e., when the Coriolis parameter, $f = f_0 + \beta y$, is set to vary linearly in space) in a non-divergent barotropic context with no background flow and no topography. Such a configuration conserves the absolute vorticity $\zeta + f$ and leads to the following equation for the relative vorticity ζ :

$$\partial_t \zeta = -\beta v - \mathbf{u} \cdot \nabla \zeta, \quad (1)$$

where v and \mathbf{u} denote the meridional and horizontal velocities. The first and second terms on the right-hand side of equation (1) are respectively linear and nonlinear. The classical view of the β -drift theory considers a Taylor expansion in time [Adem, 1956]. For an initially axi-symmetric cyclone, the first order depends only on $-\beta v$ (the nonlinear term $-\mathbf{u} \cdot \nabla \zeta$ being zero), which is positive to the west of the cyclone and negative to the east (Figure 1). This dipolar anomaly forms the so-called β gyres [Wang *et al.*, 1997]. It results in a westward tendency which corresponds to the classical westward propagation of Rossby waves. The nonlinear term appears at the second order and exhibits a poleward tendency because of the poleward velocity induced by the gyres in the center of the vortex (Figure 1). The β -drift thus reflects the nonlinear feedback of the gyres on the vortex and is due to the planetary vorticity gradient in this simple case.

[4] So far, the β -drift theory has not been tested to explain the motion of extratropical cyclones, probably because of their baroclinic structure and the dominance of linear theories in mid-latitude synoptic meteorology. However, using a two-layer quasi-geostrophic model, Gilet *et al.* [2009] showed that it affects the motion of synoptic-scale eddies when they are embedded in a baroclinically unstable zonal flow. The key parameter for the poleward shift of an extratropical surface cyclone was shown to be the vertically averaged potential vorticity (PV) gradient, which is mainly positive and poleward oriented at mid-latitudes. This parameter is an effective beta, that is, β (the planetary vorticity gradient) plus the meridional vorticity gradient associated with the jet. The

¹CNRM-GAME, Météo-France, CNRS, Toulouse, France.

²Laboratoire de Météorologie Dynamique, IPSL, ENS, CNRS, UPMC, Paris, France.

Corresponding author: G. Rivière, CNRM-GAME, Météo-France, CNRS, 42 Ave. Coriolis, F31057 Toulouse, France.

©2012. American Geophysical Union. All Rights Reserved.
0094-8276/12/2012GL052440

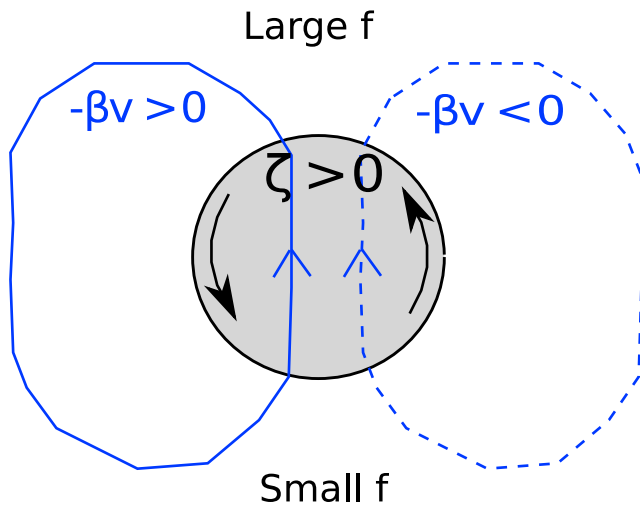


Figure 1. Schematic representation of the linear tendency term $-\beta v$ of equation (1) (blue dashed and solid lines for negative and positive values respectively) associated with an axisymmetric cyclone (gray shading) in the Northern Hemisphere. The linear tendency term presents a dipolar anomaly corresponding to the so-called beta gyres that advect the cyclone poleward (blue arrows).

purpose of the present study is to validate the key role played by the vertically averaged PV gradient (also called the barotropic PV gradient) in the evolution of a real mid-latitude surface cyclone. The approach consists in performing numerical sensitivity experiments based on the modification of the barotropic PV gradient in the initial conditions of a primitive-equation forecast model.

2. Case Study

[5] The case study concerns the storm Xynthia (26–28 February 2010), a violent wind storm that led to huge damage and many casualties in France. This was not directly related to the strong winds (gusts were not really exceptional reaching 160 km/h over the west coast of France) but rather to the generation of strong storm surges in the Bay of Biscay. The storm's track was particularly unusual, with an initial cyclone located far to the south in the central North Atlantic that moved rapidly northeastward (see its track in gray diamonds in Figure 2a). This storm is particularly relevant for our study since it moved rapidly perpendicular to the mean flow and crossed the mean jet axis over Spain. The mean jet is hereafter defined as the low-frequency (periods greater than 8 days) part of the horizontal

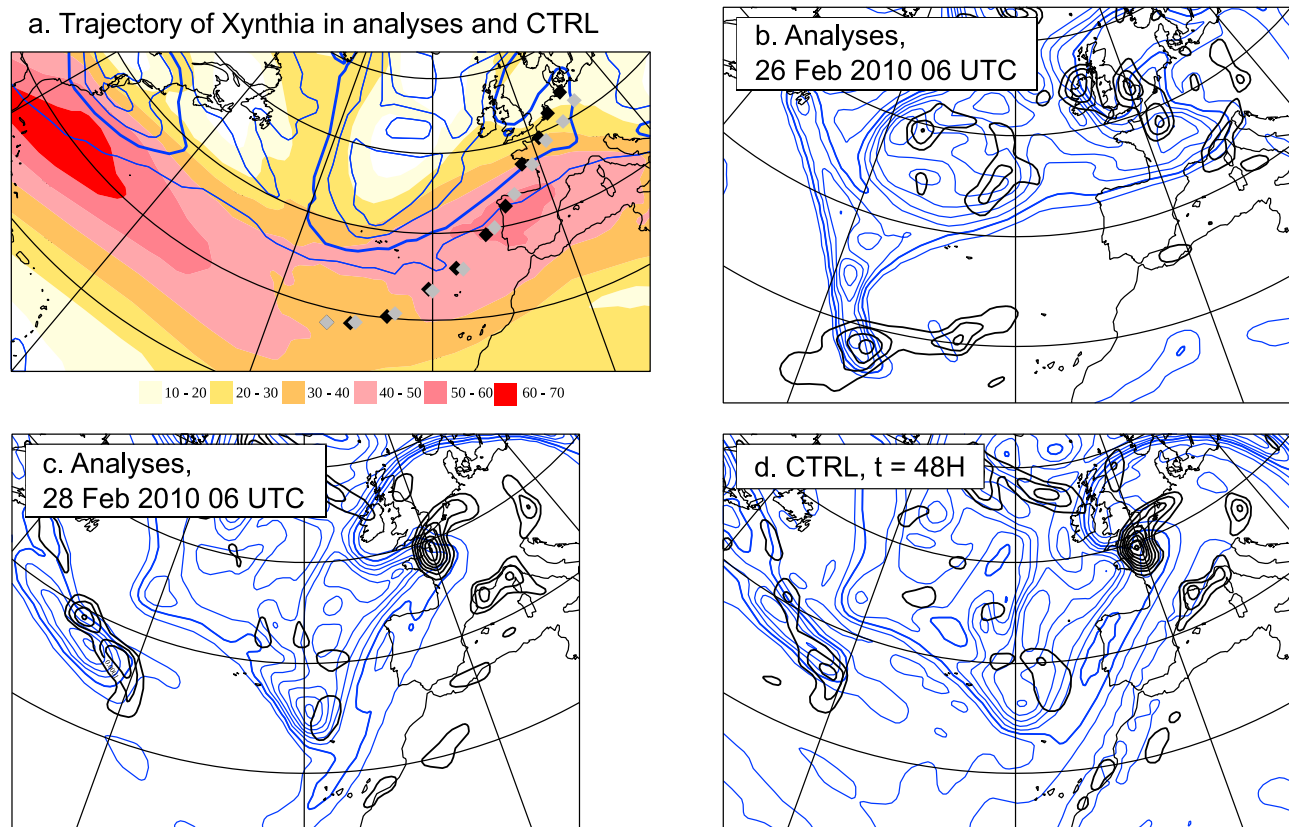


Figure 2. Description of the storm Xynthia. (a) Tracks of Xynthia shown in 6-hourly time steps between 06 UTC 26 Feb and 18 UTC 28 Feb 2010 given by the operational analysis (gray diamonds) and the 60-h control forecast starting at 06 UTC on 26 Feb (black diamonds). The blue lines correspond to the low-frequency PV (interval 1 Potential Vorticity Unit (PVU); the 2 PVU isoline is in bold) and the shading to the low-frequency wind speed (units: m s^{-1}). The tracks are computed by following the barycenter of the relative vorticity at 850 hPa. (b) Relative vorticity at 850 hPa for the operational analysis (black contours; interval: $5 \times 10^{-5} \text{ s}^{-1}$) and PV at 300 hPa (blue contours; interval 1 PVU; the 2 PVU isoline is in bold) at 06 UTC 26 Feb. (c) same as Figure 2b but at 06 UTC 28 Feb. (d) same as Figure 2b but for the control forecast after 48 hours.

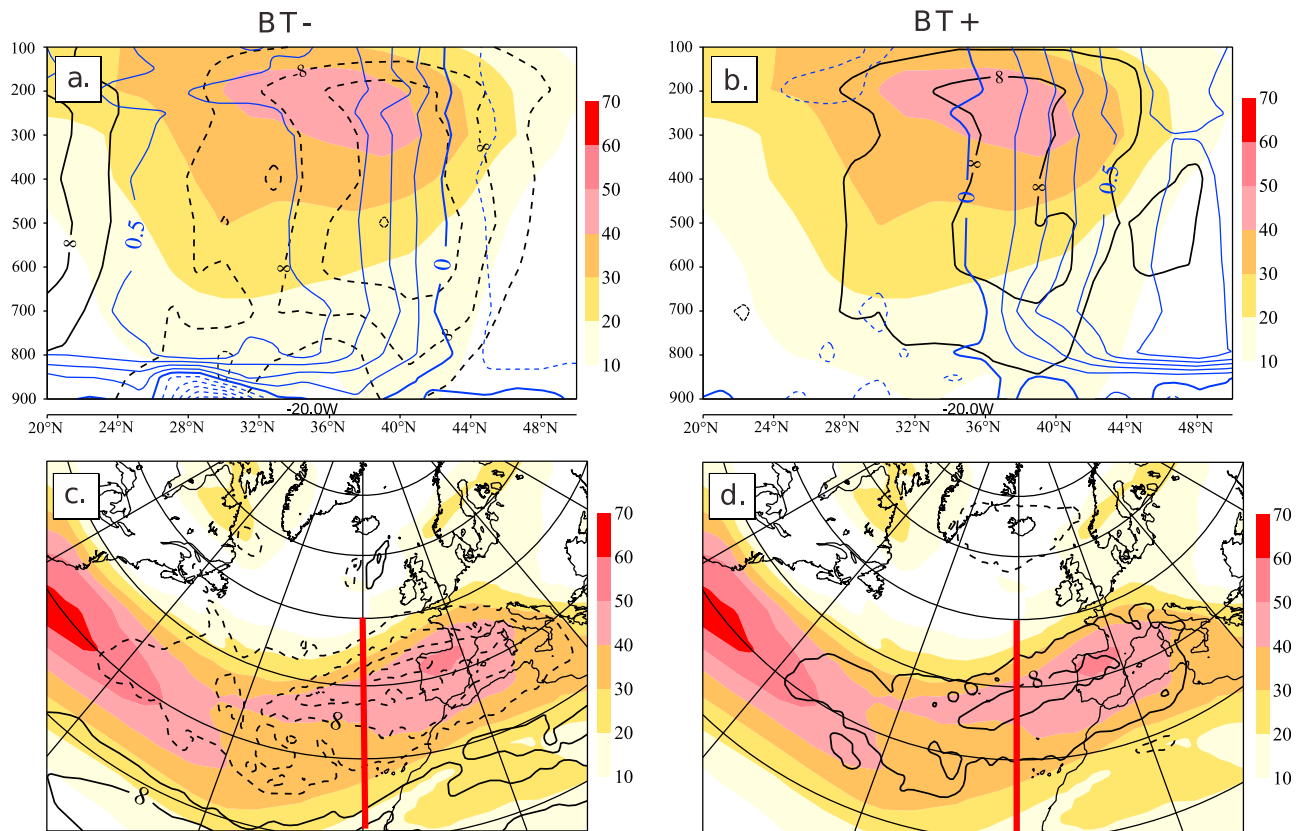


Figure 3. Initial states for BT- (Figures 3a and 3c) and BT+ (Figures 3b and 3d). (a, b) Vertical cross sections at 20° W of the zonal wind (black contours, interval 4 m s^{-1}) and PV (blue contours; interval 0.125 PVU) anomalies relative to the operational analysis at 06 UTC 26 Feb. (c, d) Longitude-latitude representation of the zonal wind anomalies at 300 hPa. The dashed and solid lines correspond to negative and positive values. In Figures 3c and 3d, the thick red lines correspond to the vertical cross sections in Figures 3a and 3b. The low-frequency zonal wind of the operational analysis is shown in shading (units: m s^{-1}).

wind in the operational analysis at 300 hPa, which does not change much during the evolution of the storm.

3. Methodology

[6] Météo-France's global primitive-equation forecast model ARPEGE-IFS [Courtier *et al.*, 1991] was used in the present study to examine the sensitivity to the barotropic PV gradient. It was run at a T798 resolution with full physics and 70 hybrid levels in the vertical. It has a stretched horizontal grid maximizing resolution over France. The 4D-Var ARPEGE operational analysis of February 2010 served as a reference for the track of Xynthia (gray diamonds in Figure 2a). A control forecast was run (hereafter denoted CTRL), starting with the operational analysis at 06 UTC on 26 February (i.e. almost 2 days before Xynthia reached France). At that time, the surface cyclone showed two relative vorticity maxima at 850 hPa to the west of the Canary Isles. The stronger one was just below an upper-tropospheric trough and the weaker one was located 10° farther downstream (Figure 2b). During its later evolution, the cyclone formed a coherent vortex with a single maximum of relative vorticity both in the analysis and in CTRL. It first stretched before crossing the upper-level jet and then suddenly contracted during the jet-crossing phase (not shown). The CTRL track (black diamonds in Figure 2a) was very close to that of the operational analysis and its sea level pressure (SLP) fell

to about 966 hPa at 06 UTC on 28 February, at the same time as the operational analysis fell to 970 hPa (not shown). At that time, the relative vorticity fields were quite close in the analysis and CTRL, with slightly larger values for the latter (Figures 2c and 2d). In both cases, the surface cyclone was just below the upper trough, creating a barotropic cyclonic structure. A strong upper-level anticyclone was created downstream, revealing a classic picture of the mature stage of a surface cyclone. Therefore, Xynthia was well captured by CTRL in comparison with the analysis.

[7] The same Ertel PV-inversion algorithm as that used in Rivière *et al.* [2010] to study the storm Lothar of December 1999 was applied here (see its detailed description in Arbogast *et al.* [2008]) to create two new experiments with two new initial states. To modify the vertically averaged PV gradient in the initial state, a barotropic PV anomaly was built starting from the low-frequency PV field at upper levels (see the blue lines in Figure 2a). The PV anomaly was then added to the PV of the operational analysis to get a new state after application of the PV-inversion tool. Two PV anomalies were constructed, one to reduce and the other to reinforce the vertically averaged PV gradient (see the auxiliary material for more details), leading to two new initial states and two new runs that are hereafter denoted as BT- and BT+ respectively.¹

¹Auxiliary materials are available in the HTML. doi:10.1029/2012GL052440.

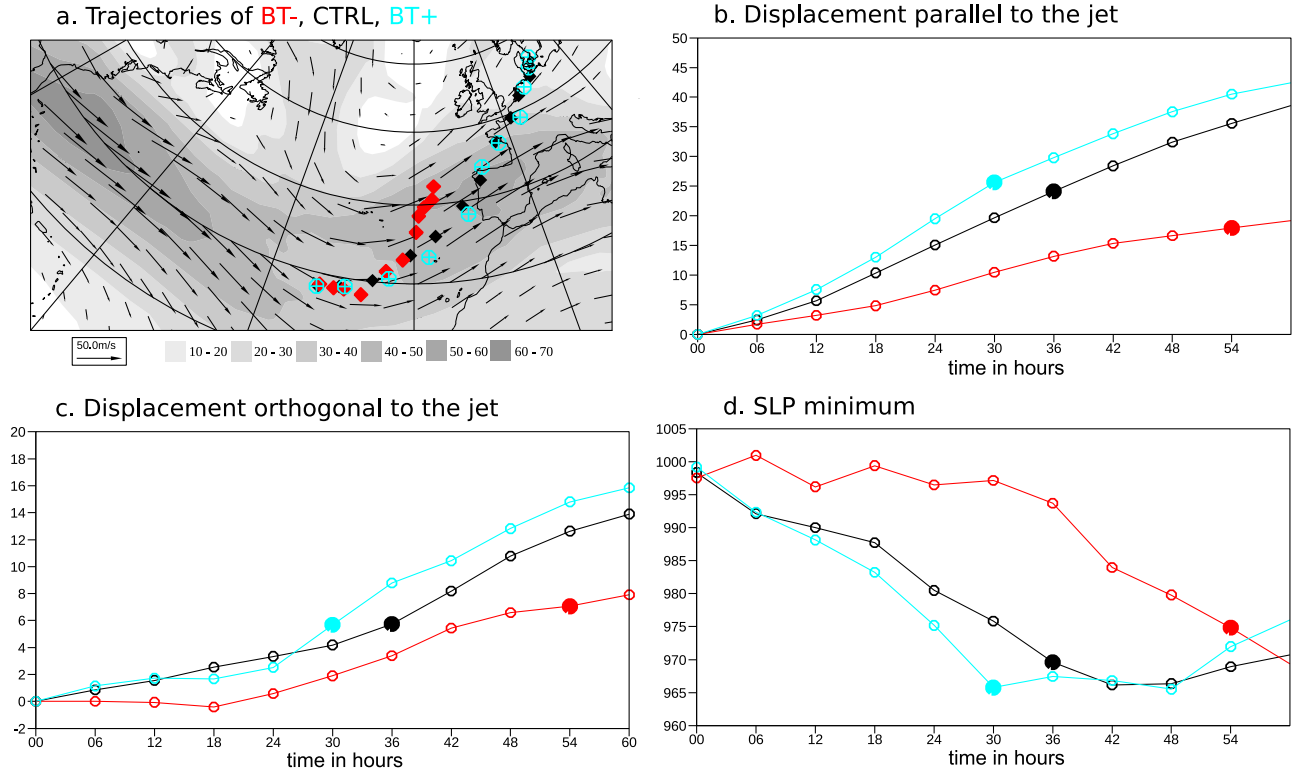


Figure 4. Motion of Xynthia in BT- (red symbols), CTRL (black symbols), BT+ (light blue symbols) runs. (a) Cyclone tracks for the three runs from $t = 0$ h to $t = 60$ h. The shading corresponds to the low-frequency wind speed (units: m s^{-1}). (b) Displacement in degrees parallel to the mean jet, $x_{||}(t)$, as a function of time. (c) Displacement in degrees perpendicular to the mean jet, $x_{\perp}(t)$, as a function of time. (d) SLP minimum. In Figures 4b–4d, the filled circles correspond to the first time the surface cyclone is on the north side of the jet.

The wind and PV anomalies after inversion for BT- and BT+ are shown in Figure 3. The gradients in PV anomaly with respect to the control case have opposite direction in BT- and BT+ (blue lines in Figures 3a and 3b), both of which have a barotropic structure from the top of the boundary layer around 850 hPa to the upper troposphere to the top of the boundary layer around 850 hPa. The zonal wind anomalies are collocated with the jet core (Figures 3a and 3b) and have a large-scale and barotropic structure with values reaching 10 m s^{-1} for BT+ and -16 m s^{-1} for BT- (Figures 3c and 3d). We therefore succeeded in building a smaller and larger vertically averaged PV gradient in BT- and BT+ compared to CTRL. Note, finally, that different tests were performed by modifying the strength and position of these anomalies to check the robustness of the following results. Generally speaking, if the amplitude of the anomalies was increased, it was checked that differences between sensitivity runs and CTRL were increased.

4. Results

[8] To diagnose the displacement of the surface cyclone relative to the mean jet, two quantities are introduced and expressed as

$$x_{||}(t) = \sum_0^t \frac{U_{lf} \Delta \lambda \cos \varphi + V_{lf} \Delta \varphi}{\sqrt{U_{lf}^2 + V_{lf}^2}}, \quad (2)$$

$$x_{\perp}(t) = \sum_0^t \frac{-V_{lf} \Delta \lambda \cos \varphi + U_{lf} \Delta \varphi}{\sqrt{U_{lf}^2 + V_{lf}^2}}. \quad (3)$$

$\Delta \lambda$ and $\Delta \varphi$ denote the displacements in longitude and latitude, respectively, of the surface cyclone within a 6-hours interval. U_{lf} and V_{lf} correspond respectively to the values of the low-frequency components of the zonal and meridional winds at 300 hPa at the location of the surface cyclone. The terms inside the sums are the displacements within 6 hours because output data sets were extracted every 6 hours. $x_{||}(t)$ and $x_{\perp}(t)$ therefore correspond to the displacement in degrees parallel and orthogonal to the mean jet respectively.

[9] The tracks of the surface cyclone in BT- and BT+ are shown in Figure 4a. For BT+ (blue symbols), the eastward motion is more rapid than in CTRL. This is confirmed more quantitatively by the computation of $x_{||}(t)$ (Figure 4b) and is in agreement with the faster large-scale westerlies in BT+. Figure 4c shows that the displacement of the surface cyclone perpendicular to the low-frequency flow is more rapid in BT+ than in CTRL after 24 hours, causing the track of BT+ to cross the jet axis sooner than the CTRL track (Figure 4a). Note that the reverse conclusions can be drawn for BT- (red symbols). We can conclude that the barotropic winds (associated with the vertically averaged PV gradient) determine the translation speed of the cyclone perpendicular to the mean jet. The fact that, in BT-, the surface cyclone did not move orthogonally to the jet axis during the first 24 hours (Figure 4c), but did move along the jet (Figure 4b), shows

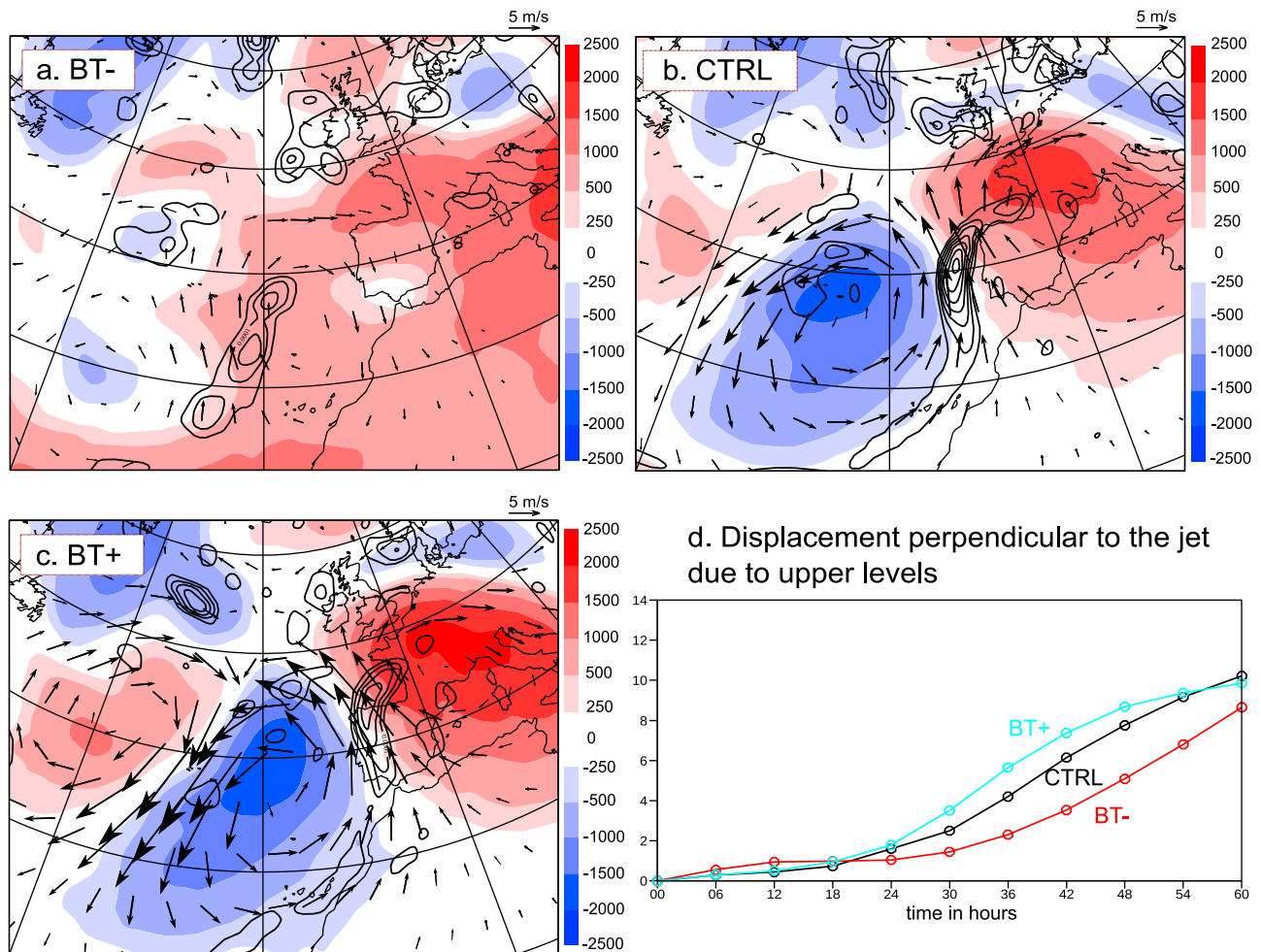


Figure 5. Upper-level anomalies in BT $^-$, CTRL, BT $^+$ and their role in Xynthia's motion. Anomalous geopotential at 300 hPa (shadings, units: $\text{m}^2 \text{s}^{-2}$), anomalous winds U_{anom} , V_{anom} and relative vorticity at 850 Pa (black contours, interval: $5 \cdot 10^{-5} \text{ s}^{-1}$) for (a) BT $^-$, (b) CTRL, (c) BT $^+$ at $t = 30 \text{ h}$. (d) Displacement in degrees perpendicular to the mean jet due to the upper-level PV dipolar anomaly, $x_{\perp}^u(t)$, as a function of time. For CTRL, the background flow from which the total flow is subtracted to get the anomaly is the low-frequency flow. For BT $^+$ and BT $^-$, the background flow is the low-frequency plus the added barotropic flow at the initial time.

that it is not the acceleration of the jet that controls the displacement of the cyclone orthogonal to the jet. Finally, once the cyclone had crossed the jet, it underwent an earlier (later) deepening phase (Figure 4d) depending on the earlier (later) crossing phase. Note that the intensities of the deepening were similar in terms of SLP minima in the three cases.

[10] Let us now identify the role of the upper-level disturbances in the cyclone motion. An upper-level trough and a ridge are located upstream and downstream, respectively, of the surface cyclone (shading in Figures 5a–5c) as in the classical picture of the baroclinic interaction between upper and lower disturbances. Our hypothesis is that this upper-level dipole may explain the motion of the surface cyclone across the mean jet axis. To verify this, anomalous winds U_{anom} , V_{anom} at 850 hPa, which can be attributed to the upper dipole, were computed after a linear inversion of the upper-level PV anomaly between 100 and 500 hPa. The poleward orientation of the wind vectors U_{anom} , V_{anom} (see the arrows in Figures 5a–5c) suggests that the upper dipole participates in the poleward advection of the surface cyclone. Furthermore, the intensity of the dipolar anomaly

and its induced winds at lower levels clearly increase from BT $^-$ to CTRL and from CTRL to BT $^+$ (Figures 5a–5c). This advection being more intense in BT $^+$ than in CTRL, the displacement orthogonal to the jet axis of the surface cyclone induced by the upper dipole is greater in BT $^+$ than in CTRL and conversely for BT $^-$. To quantify this, the following parameter was computed:

$$x_{\perp}^u(t) = \sum_0^t \frac{-V_{lf} U_{anom} + U_{lf} V_{anom}}{\sqrt{U_{lf}^2 + V_{lf}^2}} \cdot \frac{\Delta t}{a\pi/180}, \quad (4)$$

where a denotes the earth's radius and Δt the 6-hours interval. $x_{\perp}^u(t)$ corresponds to the displacement in degrees perpendicular to the mean jet that can be attributed to the upper dipole. Figure 5d confirms that $x_{\perp}^u(t)$ is smaller in BT $^-$ and greater in BT $^+$ than in CTRL. This should be compared with the real displacement orthogonal to the jet axis shown in Figure 4c. The displacement induced by upper levels $x_{\perp}^u(t)$ is slightly smaller than the real displacement $x_{\perp}(t)$ but the relative differences between the curves are similar most of

the time in Figures 4c and 5d, with more and less rapid advection for BT+ and BT−, respectively. Some discrepancies exist, however, especially at the end of the simulations (the BT+ curve being slightly below the CTRL curve in Figure 5d). To conclude, the intensity of the dipolar anomaly explains many of the differences in the motion of Xynthia perpendicular to the mean jet between BT−, CTRL and BT+.

[11] The present results can be interpreted in the light of the β -drift theory. Another view of the β -drift that complements the β -gyres picture of Figure 1 involves a vortex interaction mechanism. In presence of β , the cyclone creates an anticyclone on its eastern side via the anticyclonic tendency of the eastern gyre. This is usually called Rossby wave radiation. The circulation induced by the anticyclone advects the cyclone poleward [Oruba *et al.*, 2012]. Similarly, in the more complex baroclinic context, the stronger dipole in BT+ can be interpreted partly by the larger downstream dispersion of energy in the upper troposphere when the barotropic PV gradient is increased. This leads to a more rapid formation of the downstream upper ridge. The reverse occurs for BT−. The interpretation is confirmed by the idealized numerical experiments of Gilet *et al.* [2009, Figures 11–12] showing a more intense upper-level ridge in the case of a more intense effective β (meridional PV gradient). In other words, the proposed interpretation in a baroclinic context relies on a larger downstream dispersion of energy at upper levels in presence of a stronger effective β because it increases the positive PV gradient at these levels.

5. Conclusion

[12] The role of the vertically averaged PV gradient in the motion of a real mid-latitude storm was analyzed in the present paper and confirmed the theoretical results of Gilet *et al.* [2009]. This shows the relevance of the generalized beta drift concept in the mid-latitude baroclinic context, where the beta drift is the displacement of a vortex by a vorticity dipole generated by Rossby wave radiation. The vertically averaged PV gradient (effective β) largely determines the motion of surface extratropical cyclones perpendicular to the mean flow. The stronger the gradient, the faster the motion and the earlier the jet-crossing phase. The more intense effective β is responsible for a more efficient downstream dispersion of energy that acts to reinforce the downstream ridge which, in turn, favors the poleward advection of the surface cyclone. This interpretation will be fully detailed in a future idealized study.

[13] Let us now discuss our results relative to some observational climatological studies. Cyclones defined from conventional non-filtered atmospheric fields, such as from the minima of the geopotential height, have been shown to move poleward [Wallace *et al.*, 1988]. Kinematical arguments were provided by the authors to explain this. When a cyclone enters the storm-track region, the increased southward-oriented climatological height gradient displaces the minimum geopotential height farther to the north relative to the corresponding height anomaly. There is therefore a

significant poleward bias of the cyclone tracks when they are detected from minima of large-scale atmospheric fields such as the geopotential height or the sea level pressure. However, when a high-pass filter is used to remove this climatological mean, there is still a tendency for high-frequency minima to move poleward and across the mean climatological flow [see, e.g., Wallace *et al.*, 1988, Figure 20b] which, to the best of our knowledge, remains unexplained in the literature. This can also be observed for the tracks of relative vorticity maxima at 850 hPa [see, e.g., Hoskins and Hodges, 2002, Figure 14] to which Wallace *et al.*'s arguments cannot be applied since the relative vorticity mainly projects onto high-frequency structures and does not exhibit strong large-scale meridional gradients. Therefore, we believe that the theory of the mid-latitude beta drift provides a first dynamical interpretation for the motion of high-pass filtered cyclones across the mean climatological flow.

[14] **Acknowledgments.** This work was funded by the CNRS/INSU/LEFE/IDAO project EPIGONE.

[15] The Editor thanks the anonymous reviewer.

References

- Adem, J. (1956), A series solution for the barotropic vorticity equation and its application in the study of atmospheric vortices, *Tellus*, *8*, 364–372.
- Arbogast, P., K. Maynard, and F. Crépin (2008), Ertel potential vorticity inversion using a digital filter initialization method, *Q. J. R. Meteorol. Soc.*, *134*, 1287–1296.
- Blackmon, M. L., Y. H. Lee, and J. M. Wallace (1984), Horizontal structure of 500 mbar height fluctuations with long, intermediate and short time scales, *J. Atmos. Sci.*, *41*, 961–979.
- Carton, X. (2001), Hydrodynamical modeling of oceanic vortices, *Surv. Geophys.*, *22*, 179–263.
- Courtier, P., C. Freydl, J.-F. Geleyn, F. Rabier, and M. Rochas (1991), The ARPEGE project at Météo-France, paper presented at ECMWF Annual Seminar, Eur. Cent. for Medium-Range Weather Forecasts, Reading, U. K.
- Gilet, J.-B., M. Plu, and G. Rivière (2009), Nonlinear baroclinic dynamics of a surface cyclone crossing a zonal jet, *J. Atmos. Sci.*, *66*, 3021–3041.
- Holland, G. (1983), Tropical cyclone motion: environmental interaction plus a beta effect, *J. Atmos. Sci.*, *40*, 328–342.
- Hoskins, B. J., and K. I. Hodges (2002), A new perspective on northern hemisphere storm tracks, *J. Atmos. Sci.*, *59*, 1041–1061.
- McWilliams, J. C., and G. R. Flierl (1979), On the evolution of isolated nonlinear vortices, *J. Phys. Oceanogr.*, *9*, 1155–1182.
- Oruba, L., G. Lapeyre, and G. Rivière (2012), On the northward motion of mid-latitude cyclones in a barotropic meandering jet, *J. Atmos. Sci.*, *69*, 1793–1810.
- Pinto, J. G., S. Zacharias, A. H. Fink, G. C. Leckebusch, and U. Ulbrich (2009), Factors contributing to the development of extreme North Atlantic cyclones and their relationship with the NAO, *Clim. Dyn.*, *32*, 711–737.
- Rivière, G., and A. Joly (2006), Role of the low-frequency deformation field on the explosive growth of extratropical cyclones at the jet exit. Part I: Barotropic critical region, *J. Atmos. Sci.*, *63*, 1965–1981.
- Rivière, G., P. Arbogast, K. Maynard, and A. Joly (2010), The essential ingredients leading to the explosive growth stage of the European wind storm “Lothar” of Christmas 1999, *Q. J. R. Meteorol. Soc.*, *136*, 638–652.
- Rossby, C. G. (1948), On displacements and intensity changes of atmospheric vortices, *J. Mar. Res.*, *7*, 175–187.
- Wallace, J. M., G.-H. Lim, and M. L. Blackmon (1988), Relationship between cyclone tracks, anticyclone tracks and baroclinic waveguides, *J. Atmos. Sci.*, *45*, 439–462.
- Wang, B., X. Li, and L. Wu (1997), Direction of hurricane beta drift in horizontally sheared flows, *J. Atmos. Sci.*, *54*, 1462–1471.